Photochemical Grafting and Patterning of Biomolecular Layers onto TiO_2 Thin Films

Bo Li, Ryan Franking, Elizabeth C. Landis, Heesuk Kim, and Robert J. Hamers*

Department of Chemistry, University of Wisconsin—Madison, 1101 University Avenue, Madison, Wisconsin 53706

ABSTRACT TiO_2 thin films are highly stable and can be deposited onto a wide variety of substrate materials under moderate conditions. We demonstrate that organic alkenes will graft to the surface of TiO_2 when illuminated with UV light at 254 nm and that the resulting layers provide a starting point for the preparation of DNA-modified TiO_2 thin films exhibiting excellent stability and biomolecular selectivity. By using alkenes with a protected amino group at the distal end, the grafted layers can be deprotected to yield molecular layers with exposed primary amino groups that can then be used to covalently link DNA oligonucleotides to the TiO_2 surface. We demonstrate that the resulting DNA-modified surfaces exhibit excellent selectivity toward complementary versus noncomplementary target sequences in solution and that the surfaces can withstand 25 cycles of hybridization and denaturation in 8.3 M urea with little or no degradation. Furthermore, the use of simple masking methods provides a way to directly control the spatial location of the grafted layers, thereby providing a way to photopattern the spatial distribution of biologically active molecules to the TiO_2 surfaces. Using Ti films ranging from 10 to 100 nm in thickness allows the preparation of TiO_2 films that range from highly reflective to almost completely transparent; in both cases, the photochemical grafting of alkenes can be used as a starting point for stable surfaces with good biomolecular recognition properties.

KEYWORDS: metal oxide • photochemistry • surface functionalization • titania • DNA biointerfaces

INTRODUCTION

Titanium dioxide (TiO_2) and other metal oxides find wide use, in part, because they form spontaneously as oxidation products on metal surfaces and are very resistant to subsequent alteration (1−3). Metal oxides have been used for a range of biological applications, such as the detection of DNA (4−7). Among the metal oxides, TiO_2 has been of especially great interest because it exhibits high stability over a wide range of pH values (2, 3) and has good optical (8) and electronic properties, making it of interest for applications in sensing (8−12) and renewable energy (13−15). TiO_2 is also of importance as a naturally forming surface coating on Ti and Ti alloys that are widely used as implantable prosthetic devices (16−20); bonding of short biomolecules to the (oxidized) Ti surfaces can be used to control how cells such as osteoblasts interact with the surface (21). Previous studies have shown that thin-film coatings of materials such as diamond can produce surfaces exhibiting very high stability (22); however, the processing temperatures for diamond are high and not always compatible with common substrates such as ordinary glass. In contrast, TiO_2 can also be applied as a thin-film coating material onto glass and many other substrates at ambient or moderate temperatures as planar thin films and as highly porous films of nanocrystalline particles (23, 24), conveying improved chemical stability or high surface area to the underlying support. TiO_2 is already being applied as a thin-film coating material on glass windows on a large commercial scale (25); consequently, the development of new methods for grafting of a functional molecular layer to TiO_2 thin films may enable improved molecular and biomolecular interfaces to a range of other materials.

Several approaches have been reported previously for the grafting of molecules with various functional groups onto surfaces of TiO_2, including bonding via carboxylic acid groups (26, 27) and the use of organosilanes (28, 29). Stability of the grafted layers remains an important concern, and phosphonic acids (13, 16, 21, 30, 31) have been reported to provide enhanced stability, especially in aqueous media such as biological buffers (16, 31). However, covalent grafting of phosphonic acids is quite slow and typically involves slow evaporation of the solvent over several days at temperatures of 120 °C or higher (16, 30).

Recent studies have shown that organic alkenes can be grafted to various forms of carbon (22, 32−36) at room temperature by activating the reaction with UV light at 254 nm. The resulting layers have been used to covalently graft DNA and proteins to the surfaces, yielding bioactive layers exhibiting extremely good stability and selectivity (22, 36). In comparison, bare TiO_2 is more reactive, finding widespread use because of its ability to photochemically oxidize organic molecules (37−42). The high photochemical reactivity of TiO_2 is largely a consequence of its ability to generate reactive species such as hydroxyl radicals and superoxide (O_2^-) when in direct contact with water or oxygen (38, 43−46). Yet, the photochemical behavior of TiO_2 in contact with alkenes and other organic molecules in water- and oxygen-*deficient* environments has not been extensively explored.

Here, we show that the UV-initiated photochemical grafting of alkenes can be used to form functional molecular layers on TiO_2 thin films that can act as covalent attachment

* To whom correspondence should be addressed. E-mail: rjhamers@wisc.edu.
Received for review January 2, 2009 and accepted March 30, 2009

DOI: 10.1021/am900001h

points for DNA oligonucleotides and that the resulting DNA-modified TiO_2 surfaces exhibit excellent selectivity and stability in repeated cycles of hybridization and denaturation. We further demonstrate that the spatial location of the functional alkenes can be directly photopatterned with an edge acuity of <5 μm using a simple contact mask and that this can be extended to control the location of surface-tethered DNA oligonucleotides.

EXPERIMENTAL SECTION

Preparation of TiO_2 Films. TiO_2 films were prepared by electron-beam evaporation of Ti metal onto planar substrates followed by oxidation. Experiments reported here used (111)-oriented silicon wafers, planar borosilicate glass, and fused silica as substrates; no differences were observed between these substrates. Ti films ranging from 10 to 100 nm in thickness were deposited onto the samples and then heated at 500 °C in air for 1 h to oxidize the Ti and form a TiO_2 film. Samples prepared using the 100-nm-thick Ti were nearly opaque because the surface oxidation does not extend through the entire film, while those produced using 10 nm Ti were fully oxidized and transparent. To ensure the most reproducible surface conditions with minimal contamination, immediately before functionalization the TiO_2 samples were exposed to UV light from a low-pressure Hg lamp at 300 K for approximately 1 h in air. The UV lamp generates gas-phase ozone that cleans the surface of any residual organic contaminants and yields fully oxidized surfaces.

DNA Sequences. To explore hybridization at DNA-modified TiO_2 surfaces, we linked thio-terminated DNA oligonucleotides with two different sequences, differing by four bases, to the surface. These sequences are 5′-HS-C_6H_{12}-GC TTA TCG AGC TTT CG-3′ (S1) and 5′-HS-C_6H_{12}-GC TTA AGG AGC AAT CG-3′ (S2). DNA oligonucleotides with these sequences were modified with the 5′-thiol C6 modifier and attached to the TiO_2 surface. We explored the hybridization of these two surface-bound strands with two different sequences that were labeled with a fluorescein tag at the 5′ end. Sequence F1 (5′-FAM-CG AAA GCT CGA TAA GC-3′) is a perfect 16-base complementary match to S1, and sequence F2 (5′-FAM-CG ATT GCT CCT TAA GC-3′) is a perfect complementary match to S2, while the hybridization of S1 with F2 and S2 with F1 involves a four-base mismatch. All DNA strands were synthesized at the University of Wisconsin Biotechnology Center.

X-ray Photoelectron Spectroscopy (XPS) Characterization. XPS data were obtained on an ultrahigh-vacuum XPS system using a monochromatic Al Kα source (1486.6 eV) and a multichannel array with a resolution of 0.1−0.2 eV, collecting electrons emitted at 45° from the surface normal. Atomic area ratios were determined by fitting raw data to Voigt functions after a baseline correction and normalizing the peak area ratios by the corresponding atomic sensitivity factors [0.296 for C(1s), 0.477 for N(1s), 0.711 for O(1s), 1.0 for F(1s), and 1.798 for Ti(2p)] (47).

Fourier Transform Infrared (FTIR) Characterization. IR reflection−absorption spectra were collected on a Bruker Vector 33 FTIR spectrometer equipped with a VeeMax II variable-angle specular reflectance accessory and a wire grid polarizer. The Ti underlayer enhances the reflectance of the sample, facilitating collection of IR spectra. Spectra reported here were collected using p-polarized light with a 50° angle of incidence from the surface normal.

Fluorescence Measurements. A Genomic Systems UC4x4 fluorimager was used for all of the on-chip fluorescence intensity measurements. A 488 nm excitation source and a 512 nm bandpass filter were used for excitation and emission, respectively.

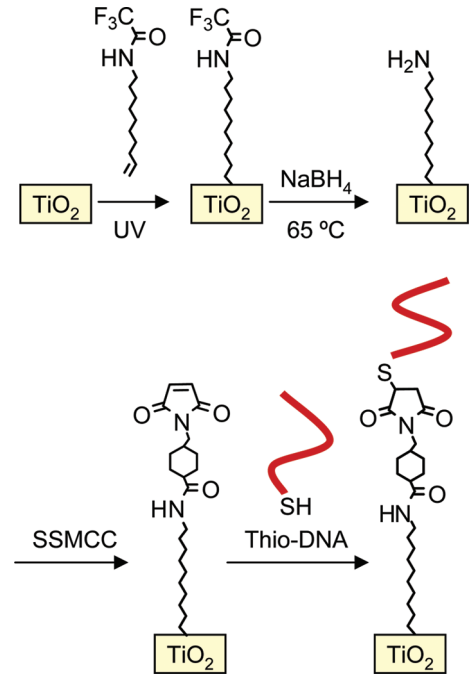

FIGURE 1. Reaction scheme of a TiO_2 film with TFAAD deprotection to produce amino-terminated surface and then reaction with a SSMCC linker and thio-DNA to produce covalently bonded DNA on the TiO_2 surface.

RESULTS

Covalent Grafting of Organic Layers to TiO_2 Surfaces. Figure 1 shows a schematic diagram of the TiO_2 surface functionalization process. The TiO_2 thin films were transferred into a N_2-purged Teflon reaction cell and covered with a thin film of N_2- or Ar-purged trifluoroacetic acid protected 10-aminodec-1-ene (TFAAD) and irradiated with UV light (254 nm and ~10 mW/cm^2) through a fused-silica window (22, 36). Control experiments were conducted using a CaF_2 window instead of fused silica, with identical results. In separate experiments (not shown), we have determined that a 15 h reaction time provides good results when starting with 100 nm Ti films, but the results are not very sensitive to the exact time used. The samples were then rinsed and soaked twice in chloroform for 5 min with ultrasonic agitation to remove any residual TFAAD. The cleaned samples were immersed in a solution of 0.024 g of $NaBH_4$ in 10 mL of anhydrous methanol at 300 K for 30 min and then refluxed for 8 h at 65 °C to deprotect the trifluoroacetic acid (TFA) protecting group. This procedure yields surfaces terminated with molecular layers bearing primary amino groups at the surface.

Figure 2 shows XPS spectra of the C(1s), F(1s), N(1s), and O(1s) regions for three samples, corresponding to a clean TiO_2 surface, a sample after grafting of the molecular layer, and a third sample after deprotection in $NaBH_4$. The clean TiO_2 sample shows only a small amount of C and no detectable F or N. After grafting of TFAAD, the C(1s) spectrum shows four peaks, similar to previous results for the TFAAD reaction onto diamond and amorphous C surfaces (36). The large peak at 283.1 eV arises from C atoms in the aliphatic chain, while a smaller shoulder at 285 eV arises from the C atom adjacent to the N atom. The peaks observed

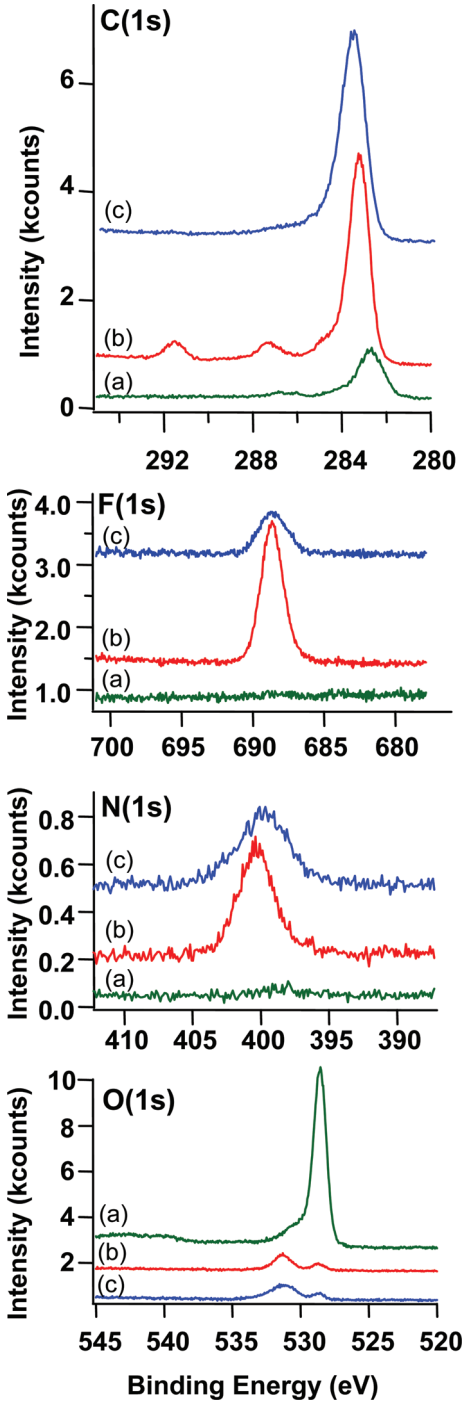

FIGURE 2. XPS C(1s), F(1s), and N(1s) spectra of the TiO_2 film. Spectra shown include (a) the clean UV-treated surface, (b) a TiO_2 sample after grafting of TFAAD, and (c) a TiO_2 sample after grafting of TFAAD and deprotection to form the primary amine.

at 287.3 and 291.5 eV are attributed to the C atom of the carbonyl (C═O) group and the C atom of the $-CF_3$ group, respectively. This spectrum closely matches a predicted spectrum based on density functional theory calculations of the one-electron orbital energies; the experimental and calculated spectra are compared in the Supporting Information. The 291.5, 287.1, 285.0, and 283.1 eV peaks are in a ratio of 1.1:1.0:2.0:12, respectively. As discussed below, the three high-binding-energy peaks are in agreement with the ratio of 1:1:2:8 expected for TFAAD bound to the surface via a C—O—Ti linkage, while the somewhat lower intensity of the aliphatic C(1s) peak at 283.1 eV likely arises from some residual contamination, observed also for the "blank" sample. Additional experiments show that gentle heating of the sample reduces the aliphatic C atom on all samples, bringing the XPS data into even better agreement with the expected values. The high-resolution F(1s) spectrum shows a peak at 688.6 eV from the TFA protecting group. The N(1s) spectrum shows a single peak at 399.3 eV from the N atom in the protected amine.

After deprotection, the C(1s) intensity at 283.1 eV is only slightly reduced, while the C(1s) peaks at 291.5 and 287.3 eV and the F(1s) peak at 688.6 eV are reduced to <~35% of their original intensity, demonstrating that >65% of the TFAAD molecules are successfully deprotected to yield primary amino groups. Deprotection leaves the N(1s) peak intensity nearly unchanged but broadened slightly and shifted to lower binding energy (from 399.3 to 399.0 eV), consistent with the removal of the electron-withdrawing TFA protecting group (22, 36, 48).

The O(1s) region initially shows a large peak at 528.6 eV, with a very small shoulder at 529.5 eV that has been attributed to TiOH groups at the surface (49). After grafting, the 528.6 eV peak is visible but is reduced in intensity, while a peak at higher binding energy, 531.3 eV, arises. The 531.3 eV peak has several contributions. Previous work showed that TFAAD grafted to diamond surfaces yielded a peak near this energy from the carbonyl group (32). Additionally, previous work showed that the Ti—O—C linkages of methoxide groups and molecularly adsorbed water both give rise to a peak ~3 eV higher in binding energy than the main O(1s) contribution from bulk TiO_2 (50). Given the size of the peak, we believe that the main contribution likely comes from physisorbed water, although contributions from the Ti—O—C molecule—surface linkage and the TFAAD molecule itself are likely.

The Ti(2p) spectrum is shown in the Supporting Information and shows no significant changes upon grafting of the molecular layer except for attenuation of the Ti photoelectrons by the organic layer. XPS peak area ratios were used to estimate the surface coverage of TFAAD molecules, with the analysis presented in the Supporting Information. Using F(1s) and C(1s) data in conjunction with the Ti(2p) bulk, we obtained values of 2×10^{15} and 1.5×10^{15} molecules/cm^2, respectively. These values are considered identical within experimental error. Both values are slightly larger than the value of 5×10^{14} molecules/cm^2 reported for self-assembled alkanethiols on Au (51); this indicates that some multilayer formation likely occurs during photochemical grafting, in agreement with previous studies on amorphous C (52). Yet, the high deprotection efficiency of >65% demonstrates that the majority of amino groups are chemically accessible.

Amino-terminated surfaces are an attractive starting point for covalent linking of biomolecules to the surface. The choice of TFAAD is dictated by the desire to have low vapor pressure (to minimize evaporation) and minimize side reactions. The use of a ~C_{10} alkyl chain provides relatively low

vapor pressure, while the TFAAD group is an attractive route toward free amino groups. We tested whether it was necessary to protect the amino group (with the TFA protecting group) by attempting to directly graft the analogous primary amine; the results (not shown) showed multiple N(1s) peaks, indicating that the TFA protecting group is necessary to achieve bonding in the desired configuration. Additional experiments (not shown) confirmed that use of the TFA protecting group significantly improves attachment of DNA to the surface.

IR Spectroscopy of Molecular Layers on TiO_2. The organic layers tethered onto the TiO_2 surface were also characterized using IR reflection−absorption spectroscopy. Figure 3a shows spectra of the photochemically grafted TFAAD layer before and after deprotection. The high-frequency region about 3200 cm^{-1} where N−H stretches are observed is obscured by water and is not shown here. Grafting of TFAAD leads to two large peaks at 2854 and 2927 cm^{-1} that are attributed to the symmetric and asymmetric CH_2 stretching vibrations, respectively. A peak at 1701 cm^{-1} is attributed to the carbonyl stretching vibration from the amide functional group (C═O), and a closely spaced grouping of three peaks at 1165, 1188, and 1211 cm^{-1} arises from the C−F vibrations of the $-CF_3$ protecting group (36, 48).

After deprotection, the most significant changes are a pronounced decrease in the intensity of the peaks from the amide (1701 cm^{-1}) and C−F (1165−1211 cm^{-1}) vibrations, while the CH_2 region (2850−2950 cm^{-1}) remains unchanged. Using the C−H modes as an internal standard, the C−F and amide peaks are reduced to ~30% of their original intensity; while IR intensities are not always proportional to concentrations, these data suggest that ~70% of the TFA protecting groups were successfully removed. The 70% deprotection yield obtained from FTIR measurements is similar to the value determined from the XPS data and confirms that the XPS data suggest that while grafting may induce some multilayer formation, the majority of TFA groups are chemically accessible. Both XPS and FTIR data show successful functionalization of TFAAD and deprotection via loss of the TFA group, leaving a surface functionalized with primary amino groups.

To gain additional insight into the molecular bonding to the surface, Figure 3b shows an enlarged view of the C−H region for TFAAD grafted onto TiO_2, along with spectra for liquid-phase TFAAD, 1-dodecene, and 1-dodecane. A pure TFAAD liquid shows peaks at 2856 and 2927 cm^{-1} from the aliphatic chain, plus weak peaks at 3106, 3078, and 2980 cm^{-1}. The slightly broadened peak at 3106 cm^{-1} has been previously assigned to an overtone of the "amide II" band (53), while the peak at 3078 cm^{-1} arises from the C−H vibrations of the terminal alkene (54). The spectrum of TFAAD grafted on TiO_2 shows large peaks at 2856 and 2727 cm^{-1} from the aliphatic chain and the weak amide II overtone peak at 3106 cm^{-1}; however, the peak at 3078 cm^{-1} from the terminal vinyl group is absent. We also note that TFAAD grafted to TiO_2 shows no evidence for methyl ($-CH_3$) stretching modes; methyl groups typically give rise to a high-frequency stretching vibration that can be clearly

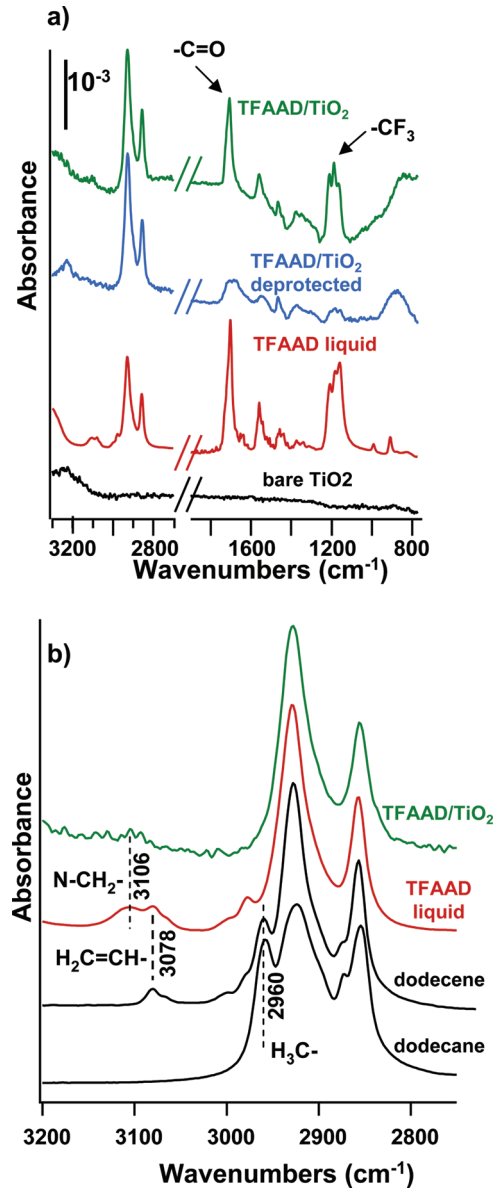

FIGURE 3. IR spectra of grafted monolayers and reactant liquids: (a) IRRAS spectra of the TiO_2 surface after UV grafting of TFAAD and the same sample after deprotection. Also shown are spectra of a pure TFAAD liquid and a "blank" sample to judge the noise level of the FTIR measurements. (b) Higher-resolution view of the C−H stretching region of TFAAD grafted onto TiO_2 and of the pure TFAAD reactant liquid. Also shown are spectra of liquid dodecane and 1-dodecene for comparison.

observed at 2960 cm^{-1} in the spectrum of dodecane (and, with roughly half the intensity, in 1-dodecene). Thus, the IR data strongly suggest that bonding to TFAAD occurs via the terminal C atom of the olefin group.

DNA Attachment and Hybridization. To link DNA oligonucleotides to the exposed amino groups, the amino-modified surfaces were exposed to a 1 mM solution of the heterobifunctional cross-linker sulfosuccinimidyl 4-(*N*-maleimidomethyl)cyclohexane-1-carboxylate (SSMCC) in a triethanolamine buffer solution (pH 7) for 2 h. The DNA oligonucleotides modified with a thiol group at the 5′ end were then linked to this surface by applying 10 μL of 250 μM thiololigonucleotide and incubating the samples in a humid reaction vessel for 9 h. Excess DNA was removed by

thorough rinsing and soaking twice in a hybridization buffer (HB, also known as a 2 × SSPE/0.2% SDS buffer, consists of 20 mM NaH_2PO_4, 300 mM NaCl, 2 mM ethylenediaminetetraacetic acid, and 7 mM sodium dodecyl sulfate, pH 7) for 10 min.

Figure 4a shows a representative fluorescence image (bright = high intensity) of a TiO_2 surface that was covalently modified with sequences S1 (left) and S2 (right). The sample was first exposed to a solution of F2 (complementary to S2, 5 μM in HB). After 5 min, the sample was rinsed, soaked twice, 10 min each, in a HB to remove nonspecifically absorbed DNA, and imaged. The top image shows an intense single spot at the location where sequence S2 was tethered to the surface, with no detectable increase in the intensity at the location where S1 was bound. This demonstrates that F2 selectively hybridizes to S2 but not to the four-base mismatched sequence S1.

To test the reversibility of hybridization, the surface was denatured in 8.3 M urea at 65 °C for 5 min, rinsed with deionized water, and imaged again; the resulting image showed no fluorescence intensity, thereby verifying complete removal of F2. The sample was then exposed to F1, following the procedure described above. Again, the appearance of the spot at the location where S1 was covalently linked demonstrated good selectivity. The sample was then exposed to a mixture of F1 and F2 after being denatured in a urea solution. As expected, the fluorescence image shows hybridization at both locations. This set of experiments shows that the DNA-modified TiO_2 surfaces exhibit excellent selectivity and reversibility, binding only to the target molecules with complementary sequences but not to molecules with noncomplementary sequences.

We evaluated the stability of surface-bound DNA oligonucleotides by characterizing the behavior during 25 repeated cycles of hybridization and denaturation. In each cycle, the sample modified with the S2 sequence was exposed to a fluorescently labeled complement (F2) for 5 min at room temperature in a humid chamber, and the intensity of fluorescence was measured after rinsing. The sample was then denatured in a 8.3 M urea solution at 65 °C for 5 min, rinsed with deionized water, and then rehybridized. The hybridization/denaturation process was performed 25 times over a period of 4 days. Between hybridization/denaturation cycles measured on different days, the sample was kept in a HB at 4 °C after denaturation. The intensity was occasionally measured after denaturation to ensure that this step removed all of the hybridized DNA between cycles. As shown in Figure 4b, the resulting fluorescence measurements showed excellent stability of the surface-bound oligonucleotides even after 25 hybridization/denaturation cycles. Some initial loss during the first few cycles is attributed to a small amount of excess S2 that was likely not covalently bound to the surface, but no significant change is observed in the later 22 cycles. This stability is similar to that reported using similar attachment chemistry on surfaces of diamond (22) and amorphous C (36). Thus, we conclude that the photochemical grafting of the initial molecular layer and the subsequent covalent DNA attachment lead to stable DNA layers with excellent selectivity and stability.

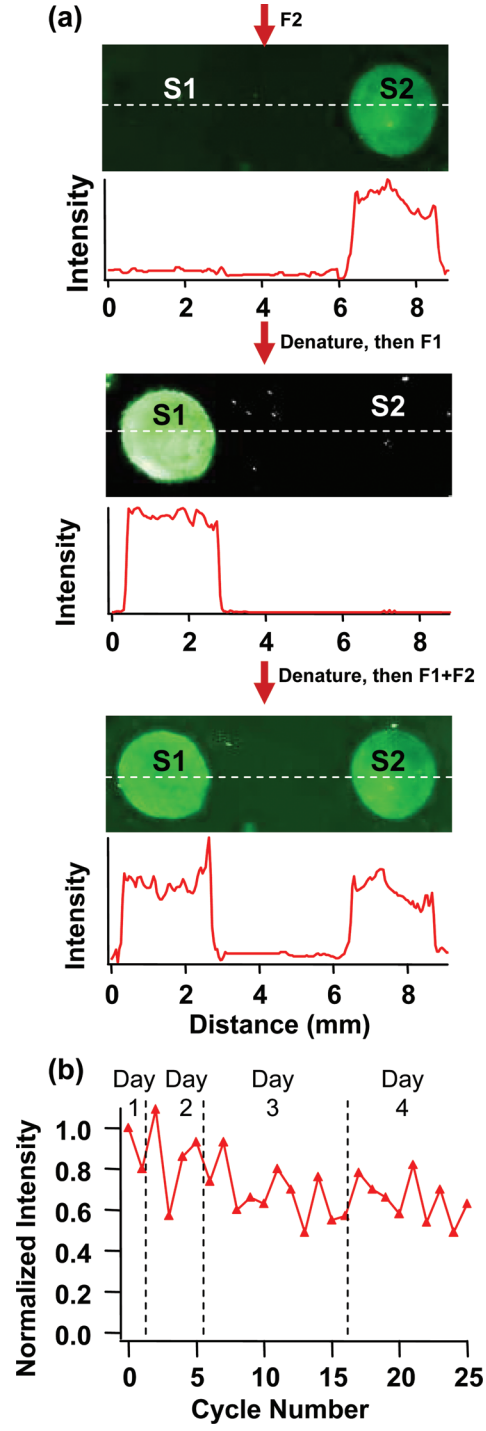

FIGURE 4. Biomolecular recognition properties of DNA-modified TiO_2: (a) Images showing the fluorescence intensity on a DNA-modified TiO_2 sample functionalized with sequences S1 and S2 and then exposed to F2 (top panels), after denaturation and exposure to F1 (middle panels), and after exposure to a mixture of F1 and F2 (bottom panels). Each measurement includes an intensity profile showing the fluorescence intensity along the indicated line. (b) Stability of a S2-modified TiO_2 surface during 25 cycles of hybridization (with F2) and denaturation over a period of 4 days, as indicated by the dashed line.

Direct Chemical Photopatterning of Molecular Functional Groups. Because the initial grafting process

is photochemical in nature, it should be possible to directly *pattern* the spatial distribution of molecules (and subsequently linked DNA oligonucleotides) onto the TiO_2 surface using a simple masking technique to control the spatial distribution of 254 nm light during the initial grafting of TFAAD. To test this ability, two types of photomasks were used here: (a) a contact mask having features with dimensions on the micron scale, fabricated using electron-beam lithography to pattern a photoresist on a UV-transmitting fused-silica substrate and then depositing Cr onto the surface via a standard "lift-off" procedure, and (b) a large-scale Cr mask with 2 mm diameter apertures. To photopattern the TiO_2 surface, a small drop of TFAAD was applied to the sample and the sample was covered with the mask, leaving a thin layer of TFAAD trapped between the sample and the mask, as depicted in Figure 5a. When this assembly was illuminated with UV (254 nm) light, the Cr-covered regions were not exposed to UV, while the open regions were exposed.

Figure 5b shows the structure of the contact mask and a SEM image of the sample after grafting of the TFAAD layer. The light-colored regions of the mask represent the transparent areas, and the black regions represent the regions blocked by the Cr layer. TFAAD was grafted to a sample using this mask and then rinsed to remove a residual organic material. Figure 5b shows the resulting SEM image of the sample, recorded using 3 kV incident electron energy and using an in-lens secondary electron detector located above the final lens of the SEM column. Similar images were also obtained using a conventional secondary electron detector in the main SEM chamber. Under the conditions used here, the regions functionalized with TFAAD appeared brighter than the unreacted TiO_2 surface, indicating that the functionalized regions have a higher secondary electron yield. The nature of molecular contrast in SEM has been discussed previously (55–57), arising primarily from changes in the local secondary electron yield. Figure 5c shows the profile of the secondary electron yield along the line depicted in Figure 5b. The profile shows that the transition from the TFAAD-modified surface (bright) to the bare TiO_2 surface (dark) is sharp, with a transition width (10–90% edge acuity) of <5 μm distance from functionalized to nonfunctionalized surface regions.

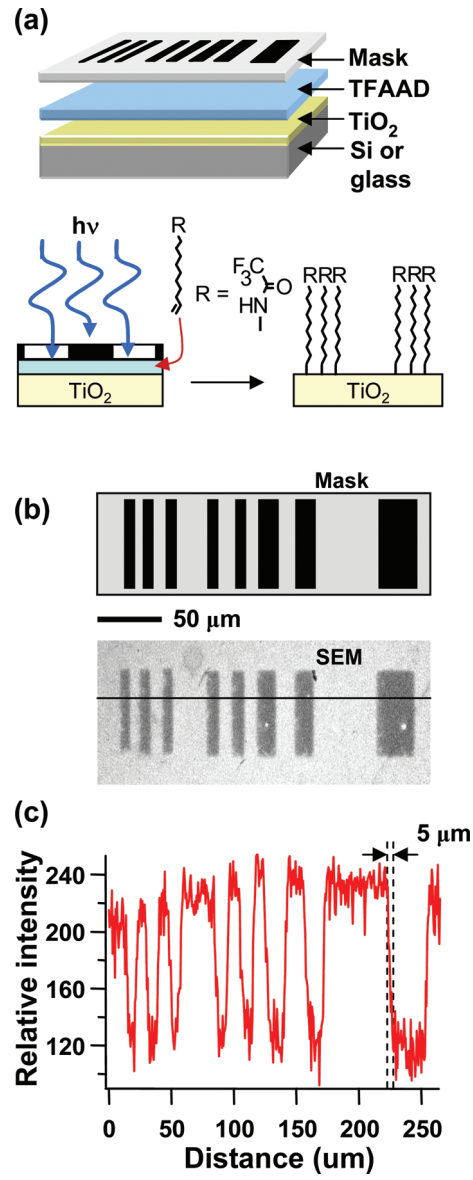

FIGURE 5. Photochemical patterning on the TiO_2 surface: (a) Top view of the original contact mask. Black represents regions blocked by Cr, and white represents regions of transparent fused silica. (b) SEM image of patterned TiO_2 surfaces. Brighter regions correspond to locations with higher secondary electron yields. (c) Profile showing the variation in the secondary electron yield along the line indicated in part b. Note the abrupt transition, <5 μm in width, between regions of high and low secondary electron yield at the positions of the vertical dotted lines.

Translation of a TFAAD Molecular Pattern into a DNA Pattern. The photopattern of TFAAD molecules can be extended to control the spatial distribution of surface-bound DNA oligonucleotides by making use of the chemical selectivity of the subsequent steps (reaction of SSMCC with the amino-terminated surface and reaction of thio-DNA with the resulting maleimide group), as depicted in Figure 6. In this case, we use a relatively large mask, with 2 mm circular transparent regions, to facilitate later analysis using a conventional fluorescence scanner. Results were obtained using both silicon and glass as starting substrates, but the results shown here were obtained using glass. A TiO_2-coated glass surface (prepared as described earlier) was first reacted with TFAAD by UV illumination through the mask and then deprotected as described above. The entire surface was then exposed to a 1 mM solution of cross-linker SSMCC for 2 h and then covered with 250 μM thiooligonucleotide (S1) for 12 h. After thorough rinsing with a HB to remove any DNA residue, the sample was exposed to a solution of F1 (complementary to S1, fluorescently labeled). Figure 6b shows the resulting fluorescence image. This figure shows intense spots at the locations illuminated with UV light, with much lower intensity at the regions where UV light was shielded by the mask. Quantitative measurement of the fluorescence intensities yields an average intensity of 6600 (arbitrary intensity units) on the DNA-grafted spots and 390 in the surrounding region. This result demonstrates that photopatterning of the

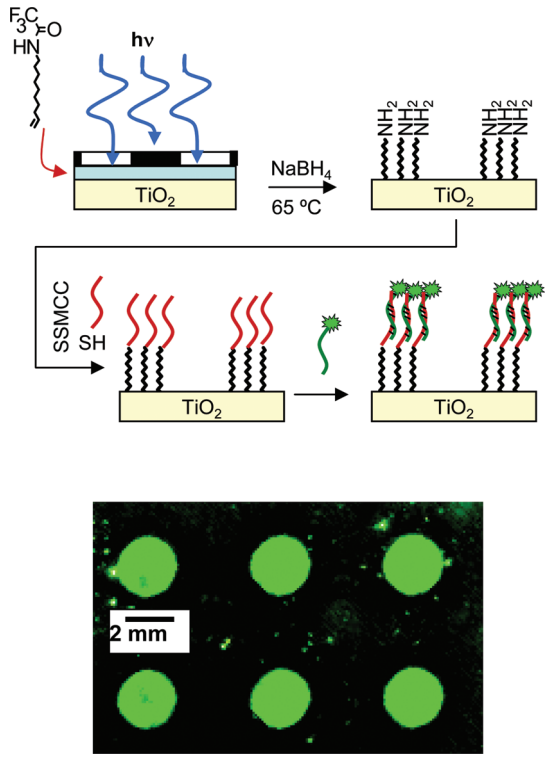

FIGURE 6. Photochemical patterning of DNA oligonucleotides onto TiO_2-coated glass: (a) Schematic of the procedure for forming patterning biomolecular layers on TiO_2. (b) Fluorescence image of a TiO_2 surface prepared by selectively grafting TFAAD to the circular regions of the sample, then exposing the entire surface to the subsequent reagents necessary to deprotect the amine, and then covalently grafting DNA S1 to the surface. The image shows the fluorescence intensity after the entire surface was exposed to the complementary sequence F1.

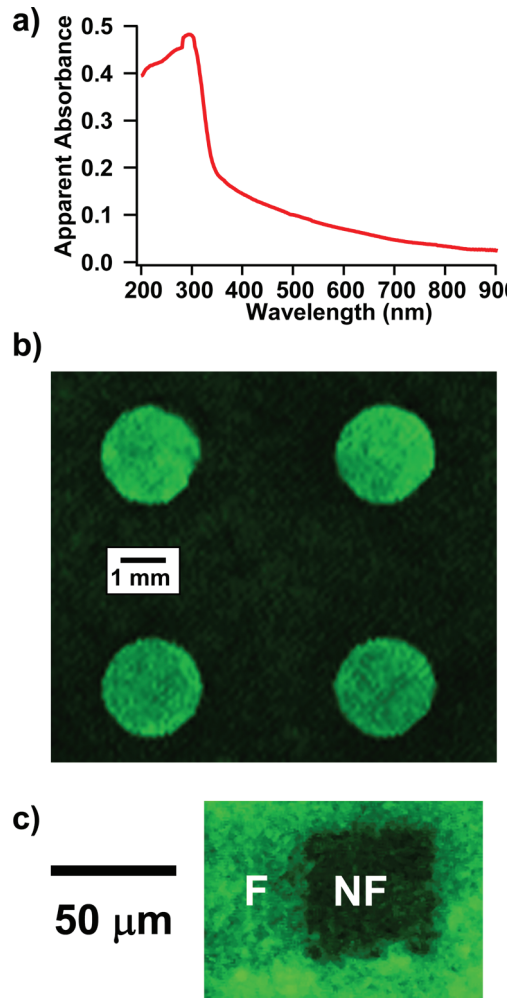

FIGURE 7. Photochemical patterning of DNA oligonucleotide thin transparent films of TiO_2 on fused silica and glass: (a) Apparent optical absorption of a TiO_2 film prepared by oxidation of a 10 nm Ti film on fused silica. (b) Fluorescence image after patterned grafting of TFAAD, followed by covalent linking of DNA to the surface and exposure to a fluorescently labeled complementary sequence. (c) Similar to part b, except at higher resolution, showing the transition of <5 μm in the intensity of fluorescence from DNA complementary sequences between surface regions that were photochemically functionalized (F) and not functionalized (NF) with TFAAD. This demonstrates faithful translation of the spatial pattern of TFAAD into the subsequent DNA layer, and the selective bonding of DNA to its complementary sequence and not to the underlying, nonfunctionalized TiO_2 regions.

TFAAD layer yields the ability to control the spatial location of biomolecular recognition groups on the surface.

Grafting of Biomolecular Layers onto Thin, Transparent TiO_2 Films. One particular feature of TiO_2 is its transparency in the visible (~400−700 nm) region of the spectrum. While the results described above were obtained using 100-nm-thick Ti films that only partially oxidize (thereby yielding relatively opaque samples), fully transparent oxide coatings can be prepared simply by using a thinner layer of Ti. Figure 7a shows the apparent absorbance of a fused-silica sample coated with 10 nm of Ti and then heated as described above to convert the Ti layer to TiO_2. The apparent absorbance, A, is defined as $A = -\log(I_{t,sample}/I_{t,reference})$ where $I_{t,sample}$ and $I_{t,reference}$ represent the intensity of light transmitted through the TiO_2-coated sample and through an identical fused-silica reference substrate, respectively. We refer to A as the *apparent* absorbance because we do not attempt to correct for changes in surface reflection losses between the TiO_2-coated sample and the reference sample. The onset of absorption below 350 nm (3.5 eV) and the overall shape of the absorption spectrum are consistent with the known absorption spectrum of TiO_2 thin films (58). As described in the Supporting Information, the apparent absorption in the 900−400 nm region is consistent with the expected increase in the wavelength-dependent *reflectivity* of the sample (which is indistinguishable from absorption in a simple transmission experiment), due to the high index of refraction of TiO_2. A more detailed analysis of the absorption spectrum (59), presented in the Supporting Information, indicates that the TiO_2 thin film has an indirect band gap of 3.05 eV and a direct band gap of 3.64 eV. The indirect gap of 3.05 eV is, within experimental error, equal to the band gap of crystalline TiO_2 in the rutile (3.03 eV) and anatase (3.18 eV) phases (58).

Figure 7b shows results obtained by depositing a 10 nm film of Ti, oxidizing as above, photopatterning a layer of TFAAD onto the surface, and then grafting DNA onto the surface. The samples were then exposed to fluorescently labeled cDNA. Using the mask with 2 mm apertures, the resulting pattern of DNA is again clearly visible. Under the conditions of this experiment, we observed a background

signal of 1890 (arbitrary intensity units) on a "bare" TiO_2 never exposed to fluorescent DNA; this reflects the detector dark current and imperfect rejection of reflected light at the wavelength of interest. On the sample that was modified with DNA, the intensity is increased to 4640 (an increase of 2750) on the nonfunctionalized regions of the TiO_2 and 8340 on the DNA-modified regions (an increase of 6450). These results demonstrate that there is some nonspecific binding of DNA to the TiO_2-modified surface; however, the overall fluorescence yield appears to be similar to that of the thicker films. Experiments were also conducted using a mask with smaller feature sizes to test the sharpness of the transition from functionalized to nonfunctionalized regions. A high-resolution fluorescence image of a pattern produced using a Cr mask with small features in Figure 7c shows a sharp (10−90% intensity transition occurring over a distance of $<5\ \mu$m) boundary between the functionalized (F) and nonfunctionalized (NF) regions of the sample, although some heterogeneity is observed on this length scale. This transition is similar in width to that observed for the initial molecular layer (Figure 5), demonstrating that the pattern produced in the initial layer is faithfully translated into the pattern of surface-bound DNA oligonucleotides.

DISCUSSION

The above results show that the use of photochemical grafting provides an effective method for conveying biomolecular recognition properties to TiO_2 thin films. The data show that DNA-modified TiO_2 surfaces produced in this manner exhibit stability comparable to that reported previously from amorphous C (36) and diamond (22) substrates. These results suggest that photochemical grafting onto TiO_2 thin films, both as surface oxides on Ti metals/alloys and as thin transparent films, may be an effective way of conveying specific types of biomolecular recognition or other biological activity (e.g., reduction in nonspecific binding via use of ethylene glycol oligomers) (60, 61) to surfaces.

While the detailed mechanism on TiO_2 has not yet been determined, previous studies have shown that UV excitation will induce alkenes to graft onto hydrogen-terminated silicon surfaces and have proposed that it occurs via an an exciton process in which the positively charged holes react with the electron-rich alkenes (62, 63). We propose that a somewhat similar process is likely on TiO_2. Absorption of above-band-gap light by TiO_2 creates electron−hole pairs; the electrons are known to be captured by Ti^{4+} ions, while the holes are captured by O atoms or surface hydroxyl groups (64, 65) that are commonly present on TiO_2 surfaces. Gas-phase studies show that interaction of alkenes with TiO_2 produces desorption of saturated alkenes (e.g., ethane) (64, 66) when surface −OH groups are present, with the −OH groups serving as the source of H. It is likely that grafting of TFAAD occurs in a similar manner: the O atom of a surface −OH group binds to an unsaturated C═C atom, and the H atom transfers to the adjacent C atom to form a covalently saturated surface adduct. Such a reaction would be expected to be self-limiting because of the finite number of H atoms present as surface −OH groups.

Studies of the resulting gas-phase product distributions have shown that the illuminated TiO_2 interacts preferentially with the terminal $=CH_2$ group (i.e., the α-C) rather than the $=CH-$ group (the β-C). These can be distinguished by the fact that if the hydroxyl O atom binds to the terminal (α) H, then the resulting alkyl chain will consist only of CH_2 groups, while if the O atom binds at the β-C, then transfer of the H atom from −OH to the molecule produces a $-CH_3$ group. While not definitive, our data in Figure 3b do not show evidence for any $-CH_3$ groups on the TFAAD-grafted surface. This mode of bonding is often referred to as "anti-Markovnikov" addition (67).

One surprising aspect of our work is that many previous studies have shown that TiO_2 is an efficient photocatalyst for degrading organic compounds (37, 38, 40, 41). In these photocatalytic applications, however, the photoinduced reactions result in products that *leave* the TiO_2 surface, while our grafting reaction leads to layers that are *bound stably* to the surface. We believe a key factor in obtaining stable monolayers is that, by exclusion of water and O atoms during the grafting reaction, the only H available for reaction comes from the surface −OH groups (68). In photocatalytic reactions, the reactants are typically dispersed in oxygenated aqueous media, where UV excitation creates highly reactive oxygen-containing species such as hydroxyl radical $HO^{\bullet}$ (40), superoxide (O_2^-) (38), and excited oxygen $O(^3P)$ (38) from surface-adsorbed water and O_2. Our results suggest that in the absence of water or O atoms the photochemical reaction of TiO_2 with alkenes leads to molecular layers covalently bonded to the TiO_2 surface. Indeed, in separate experiments, we have found that the presence of water and O atoms can lead to polymerization and other side reactions, while exclusion of water and O atoms leads to self-limiting surface reactions. While the photoactive capability of TiO_2 could potentially lead to photooxidation of grafted layers if they are illuminated with UV light with wavelengths shorter than 400 nm, for many applications (including most biological fluorescence imaging experiments), this can be easily avoided. We have not detected any significant degradation while working in a laboratory environment with ordinary fluorescent lights and have successfully stored DNA-modified samples for several months with no detectable degradation upon subsequent hybridization experiments.

More detailed studies will be required to establish a definitive reaction mechanism and structure. Yet, the data presented here demonstrate that TiO_2 can be used as a thin transparent coating that can be easily functionalized with DNA and/or other molecules of interest. The ability to covalently link biomolecules to TiO_2 may be important for applications such as Ti-based prosthetic implants, where control of protein adsorption is critical to mitigating inflammatory response and enhancing biocompatibility (20, 69−72). Transparent oxides prepared by the oxidation of Ti or by other processes such as sputter deposition (73, 74) may be advantageously applied as a means to covalently link and photopattern biomolecules onto glass, plastic, and other transparent materials. The use of Ti metal as a starting point

for TiO_2 formation is particularly convenient because Ti is easy to deposit and exhibits excellent adhesion to a wide range of materials (75, 76). Through control of the thickness of the film and the oxidation conditions, it is possible to prepare highly reflective surfaces or transparent surfaces.

On films prepared using thin Ti layers, additional experiments suggest that the grafting efficiency is only slightly lower that that obtained on thicker films, even though the fraction of light absorbed is smaller. As described in the Supporting Information, the apparent absorption in the 400−900 nm range of Figure 7a is consistent with the wavelength-dependent *surface reflection* loss due to the high index of refraction of TiO_2. On the basis of the observed reflection loss in the 400−900 nm range, we estimate that at 254 nm the total (apparent) absorbance of 0.4 consists of a true absorbance of ~0.2 combined with a reflection loss. A true absorbance of 0.2 represents ~37% of the incident light being absorbed. While a lower efficiency of grafting may be expected on very thin TiO_2 films due to incomplete absorption of all of the incident 254 nm light, our results suggest only small differences. This suggests that the reaction may be limited by surface or near-surface excitations rather than bulk excitations. Other factors, such as the inability of very thin films to support a charge-separating space-charge layer, may also contribute to the grafting efficiency. Overall, however, it is clear that even very thin films can be successfully used for grafting of biomolecular layers.

CONCLUSION

We have demonstrated that organic alkenes will graft to the surface of TiO_2 when illuminated with UV light at 254 nm and that the resulting surfaces can serve as a starting point for the preparation of DNA-modified TiO_2 thin films exhibiting excellent stability and selectivity. The ability to easily form thin TiO_2 films on a wide variety of substrates at or near room temperature suggests that the photochemical functionalization and subsequent covalent linking procedures outlined here may provide a versatile and simple method for conveying highly selective and stable biomolecular recognition properties to a wide variety of substrate materials, including Ti metal alloys, glass, and polymers.

Acknowledgment. This work is supported, in part, by the National Science Foundation Grant CHE-0613010, DMR-0425880, and the Army Environmental Quality Program of the U.S. Army Corp of Engineers. E.C.L. thanks the Merck Co. for a Merck Graduate Fellowship.

Supporting Information Available: XPS spectrum of the Ti(2p) region before and after grafting of a TFAAD molecular layer; details of the estimation of molecular coverage from XPS data; simulated C(1s) XPS spectrum; analysis of the optical absorption spectrum of a TiO_2 thin film prepared by the oxidation of a 10-nm-thick Ti layer. This material is available free of charge via the Internet at http://pubs.acs.org.

REFERENCES AND NOTES

(1) Knauss, K. G.; Dibley, M. J.; Bourcier, W. L.; Shaw, H. F. *Appl. Geochem.* **2001**, *16*, 1115.
(2) Ziemniak, S. E.; Jones, M. E.; Combs, K. E. S. *J. Solution Chem.* **1993**, *22*, 601.
(3) Ziemniak, S. E.; Opalka, E. P. *Chem. Mater.* **1993**, *5*, 690.
(4) Kumar, N.; Dorfman, A.; Hahm, J. I. *Nanotechnology* **2006**, *17*, 2875.
(5) Dorfman, A.; Kumar, N.; Hahm, J.-i. *Langmuir* **2006**, *22*, 4890.
(6) Taratula, O.; Galoppini, E.; Mendelsohn, R.; Reyes, P. I.; Zhang, Z.; Duan, Z.; Zhong, J.; Lu, Y. *Langmuir* **2009**, *25*, 2107.
(7) Zhao, J. W.; Wu, L. Z.; Zhi, J. F. *J. Mater. Chem.* **2008**, *18*, 2459.
(8) Sirbuly, D.; Law, M.; Yan, H.; Yang, P. *J. Phys. Chem. B* **2005**, *109*, 15190.
(9) Doong, R.; Shih, H. *Biosens. Bioelectron.* **2006**, *22*, 185.
(10) Lu, W.; Wang, G.; Jin, Y.; Yao, X.; Hu, J.; Li, J. *Appl. Phys. Lett.* **2006**, 89.
(11) Liu, J.; Roussel, C.; Lagger, G.; Tacchini, P.; Girault, H. *Anal. Chem.* **2005**, *77*, 7687.
(12) Tokudome, H.; Yamada, Y.; Sonezaki, S.; Ishikawa, H.; Bekki, M.; Kanehira, K.; Miyauchi, M. *Appl. Phys. Lett.* **2005**, 87.
(13) Galoppini, E. *Coord. Chem. Rev.* **2004**, *248*, 1283.
(14) Gratzel, M. *Inorg. Chem. Commun.* **2005**, *44*, 684.
(15) Gratzel, M. *C. R. Chim.* **2006**, *9*, 578.
(16) Adden, N.; Gamble, L. J.; Castner, D. G.; Hoffmann, A.; Gross, G.; Menzel, H. *Langmuir* **2006**, *22*, 8197.
(17) Viornery, C.; Chevolot, Y.; Leonard, D.; Aronsson, B. O.; Pechy, P.; Mathieu, H. J.; Descouts, P.; Gratzel, M. *Langmuir* **2002**, *18*, 2582.
(18) Huang, N. P.; Michel, R.; Voros, J.; Textor, M.; Hofer, R.; Rossi, A.; Elbert, D. L.; Hubbell, J. A.; Spencer, N. D. *Langmuir* **2001**, *17*, 489.
(19) Hofer, R.; Textor, M.; Spencer, N. D. *Langmuir* **2001**, *17*, 4014.
(20) Schliephake, H.; Scharnweber, D. *J. Mater. Chem.* **2008**, *18*, 2404.
(21) Gawalt, E. S.; Avaltroni, M. J.; Danahy, M. P.; Silverman, B. M.; Hanson, E. L.; Midwood, K. S.; Schwarzbauer, J. E.; Schwartz, J. *Langmuir* **2003**, *19*, 200.
(22) Yang, W. S.; Auciello, O.; Butler, J. E.; Cai, W.; Carlisle, J. A.; Gerbi, J. E.; Gruen, D. M.; Knickerbocker, T.; Lasseter, T. L.; Russell, J. N., Jr.; Smith, L. M.; Hamers, R. J. *Nat. Mater.* **2002**, *1*, 253.
(23) Kozhukharov, V.; Trapalis, C.; Samuneva, B. *J. Mater. Sci.* **1993**, *28*, 1283.
(24) Hagfeldt, A.; Gratzel, M. *Chem. Rev.* **1995**, *95*, 49.
(25) Werner, A.; Roos, A. *Sol. Energy Mater. Sol. Cells* **2007**, *91*, 609.
(26) Marguerettaz, X.; Oheill, R.; Fitzmaurice, D. *J. Am. Chem. Soc.* **1994**, *116*, 2629.
(27) Heimer, T.; DArcangelis, S.; Farzad, F.; Stipkala, J.; Meyer, G. *Inorg. Chem.* **1996**, *35*, 5319.
(28) Tanaka, T.; Hatakeyama, K.; Sawaguchi, M.; Iwadate, A.; Mizutani, Y.; Sasaki, K.; Tateishi, N.; Takeyama, H.; Matsunaga, T. *Biotechnol. Bioeng.* **2006**, *95*, 22.
(29) Oliveira, E.; Beyer, S.; Heinze, J. *Bioelectrochemistry* **2007**, *71*, 186.
(30) Gawalt, E. S.; Avaltroni, M. J.; Koch, N.; Schwartz, J. *Langmuir* **2001**, *17*, 5736.
(31) Mani, G.; Johnson, D.; Marton, D.; Dougherty, V.; Feldman, M.; Patel, D.; Ayon, A.; Agrawal, C. *Langmuir* **2008**, *24*, 6774.
(32) Nichols, B.; Butler, J.; Russell, J.; Hamers, R. *J. Phys. Chem. B* **2005**, *109*, 20938.
(33) Strother, T.; Knickerbocker, T.; Russell, J.; Butler, J.; Smith, L.; Hamers, R. *Langmuir* **2002**, *18*, 968.
(34) Zhong, Y.; Chong, K.; May, P.; Chen, Z.; Loh, K. *Langmuir* **2007**, *23*, 5824.
(35) Baker, S. E.; Tse, K. Y.; Hindin, E.; Nichols, B. M.; Clare, T. L.; Hamers, R. J. *Chem. Mater.* **2005**, *17*, 4971.
(36) Sun, B.; Colavita, P.; Kim, H.; Lockett, M.; Marcus, M.; Smith, L.; Hamers, R. *Langmuir* **2006**, *22*, 9598.
(37) Augustynski, J. *Electrochim. Acta* **1993**, *38*, 43.
(38) Fan, J. F.; Yates, J. T. *J. Am. Chem. Soc.* **1996**, *118*, 4686.
(39) Gerischer, H.; Heller, A. *J. Phys. Chem.* **1991**, *95*, 5261.
(40) Carp, O.; Huisman, C. L.; Reller, A. *Prog. Solid State Chem.* **2004**, *32*, 33.
(41) Kormann, C.; Bahnemann, D. W.; Hoffmann, M. R. *Environ. Sci. Technol.* **1991**, *25*, 494.
(42) Guillard, C.; Debayle, D.; Gagnaire, A.; Jaffrezic, H.; Herrmann, J. M. *Mater. Res. Bull.* **2004**, *39*, 1445.
(43) Lu, G. Q.; Linsebigler, A.; Yates, J. T. *J. Chem. Phys.* **1995**, *102*, 4657.
(44) Thompson, T. L.; Yates, J. T. *Chem. Rev.* **2006**, *106*, 4428.
(45) Linsebigler, A. L.; Lu, G. Q.; Yates, J. T. *Chem. Rev.* **1995**, *95*, 735.

(46) Henderson, M. A.; Epling, W. S.; Peden, C. H. F.; Perkins, C. L. *J. Phys. Chem. B* **2003**, *107*, 534.
(47) Moulder, J. F.; Stickle, W. F.; Sobol, P. E.; Bomben, K. D. *Handbook of X-ray Photoelectron Spectroscopy*; Physical Electronics Division, Perkin-Elmer Corp.: Waltham, MA, 1992.
(48) Kim, H.; Colavita, P.; Metz, K.; Nichols, B.; Sun, B.; Uhlrich, J.; Wang, X.; Kuech, T.; Hamers, R. *Langmuir* **2006**, *22*, 8121.
(49) Lu, G.; Bernasek, S. L.; Schwartz, J. *Surf. Sci.* **2000**, *458*, 80.
(50) Herman, G. S.; Dohnalek, Z.; Ruzycki, N.; Diebold, U. *J. Phys. Chem. B* **2003**, *107*, 2788.
(51) Nuzzo, R.; Allara, D. *J. Am. Chem. Soc.* **1983**, *105*, 4481.
(52) Colavita, P.; Streifer, J.; Sun, B.; Wang, X.; Warf, P.; Hamers, R. *J. Phys. Chem. C* **2008**, *112*, 5102.
(53) McLachlan, R. D.; Nyquist, R. A. *Spectrochim. Acta* **1964**, *20*, 1397.
(54) Zakharieva, O.; Forster, H.; Turneva, M. *Spectrochim. Acta* **1994**, *50A*, 19.
(55) Saito, N.; Wu, Y.; Hayashi, K.; Sugimura, H.; Takai, O. *J. Phys. Chem. B* **2003**, *107*, 664.
(56) Mack, N. H.; Dong, R.; Nuzzo, R. G. *J. Am. Chem. Soc.* **2006**, *128*, 7871.
(57) Wang, X.; Colavita, P.; Metz, K.; Butler, J.; Hamers, R. *Langmuir* **2007**, *23*, 11623.
(58) Kumar, P. M.; Badrinarayanan, S.; Sastry, M. *Thin Solid Films* **2000**, *358*, 122.
(59) Pankove, J. I. *Optical processes in semiconductors*; Dover Publications, Inc.: New York, 1971.
(60) Lasseter Clare, T.; Clare, B. H.; Nichols, B. M.; Abbott, N. L.; Hamers, R. J. *Langmuir* **2005**, *21*, 6344.
(61) Lasseter, T. L.; Clare, B. H.; Abbott, N. L.; Hamers, R. J. *J. Am. Chem. Soc.* **2004**, *126*, 10220.
(62) Stewart, M. P.; Buriak, J. M. *J. Am. Chem. Soc.* **2001**, *123*, 7821.
(63) Stewart, M. P.; Maya, F.; Kosynkin, D. V.; Dirk, S. M.; Stapleton, J. J.; McGuiness, C. M.; Allara, D.; Tour, J. M. *J. Am. Chem. Soc.* **2004**, *126*, 370.
(64) Boonstra, A. H.; Mutsaers, C. A. H. A. *J. Phys. Chem.* **1975**, *79*, 2025.
(65) Anpo, M. *Res. Chem. Intermed.* **1989**, *11*, 67.
(66) Kodama, S.; Yagi, S. *J. Phys. Chem.* **1989**, *93*, 4556.
(67) Smith, M. B.; March, J. *March's advanced organic chemistry: Reactions, mechanisms, and structure*, 5th ed.; John Wiley & Sons, Inc.: New York, 2001.
(68) Anpo, M.; Aikawa, N.; K., Y. *J. Phys. Chem.* **1984**, *88*, 3998.
(69) Liu, Q.; Ding, J.; Mante, F. K.; Wunder, S. L.; Baran, G. R. *Biomaterials* **2002**, *23*, 3103.
(70) Castner, D. G.; Ratner, B. D. *Surf. Sci.* **2002**, *500*, 28.
(71) Ratner, B. D. *J. Mol. Recognit.* **1996**, *9*, 617.
(72) Albrektsson, T.; Branemark, P. I.; Hansson, H. A.; Lindstrom, J. *Acta Orthop. Scand.* **1981**, *52*, 155.
(73) Dannenberg, R.; Greene, P. *Thin Solid Films* **2000**, *360*, 122.
(74) Pan, J.; Leygraf, C.; Thierry, D.; Ektessabi, A. M. *J. Biomed. Mater. Res.* **1997**, *35*, 309.
(75) Hahner, G.; Hofer, R.; Klingenfuss, I. *Langmuir* **2001**, *17*, 7047.
(76) Busch, G.; Jaehne, E.; Cai, X. D.; Oberoi, S.; Adler, H. J. P. *Synth. Met.* **2003**, *137*, 871.

AM900001H